



Published in final edited form as:

J Immunol. 2010 May 1; 184(9): 5242–5252. doi:10.4049/jimmunol.0903319.

ICAM-1 enrichment near tri-cellular endothelial junctions is preferentially associated with leukocyte transmigration, and signals for reorganization of these junctions to accommodate leukocyte passage

Ronen Sumagin* and Ingrid H Sarelius*

*Department of Pharmacology and Physiology, University of Rochester, Rochester, New York

Abstract

Leukocyte transmigration occurs at specific locations (portals) on the endothelium, but the nature of these portals is not clear. Using intravital confocal microscopy of anesthetized mouse cremaster muscle in combination with immunofluorescence labeling, we showed that in microvessels transmigration is mainly junctional and preferentially occurs at tri-cellular endothelial junctional regions. Our data suggest that enrichment of ICAM-1 near approximately 43% of these junctions makes these locations preferred for transmigration, by signaling the location of a nearby portal, as well as preparing the EC-junctions to accommodate leukocyte passage. Blockade of the extracellular domain of the ICAM-1 significantly reduced transmigration (by 68.8±4.5%), by reducing the ability of leukocytes to get to these portals. In contrast, blockade of the cytoplasmic tail of ICAM-1 reduced transmigration (by 71.1±7.0%) by disabling VE-Cadherin rearrangement. Importantly, venular convergences are optimally equipped to support leukocyte transmigration. Differences in EC morphology result in a significantly higher number of tri-cellular junctions in convergences compared to straight venular regions (20.7±1.2 vs 12.43±1.1/6000µm², respectively). Consequently leukocyte adhesion and transmigration are significantly higher in convergences compared to straight regions (1.6- and 2.6-fold, respectively). Together, these data identify an important role for EC morphology and expression patterns of ICAM-1 in leukocyte transmigration.

Keywords

leukocyte; trafficking; crawling; transmigration; adhesion molecules; VE-Cadherin; in-vivo

Introduction

Leukocyte extravasation is a complex multistep process that requires overlapping function of both leukocytes and endothelial cells (ECs). Each step has been extensively studied and is elegantly summarized in recent reviews (1-4). To effectively exit the blood vessels, leukocytes initiate rolling contacts with endothelium (5), followed by firm adhesion (6). Leukocyte rolling is primarily mediated by interactions between members of the selectin family and the glycosylated molecules expressed on the leukocyte surface (7). Leukocyte adhesion is mainly mediated by interactions between members of CAM family, such as ICAM-1, and their counter

Address for Correspondence: Ingrid H. Sarelius, Ph.D., Dept. Pharmacology and Physiology, University of Rochester Medical Center, 601 Elmwood Ave, Rochester, NY 14642, Phone: 585 275 7729, Fax: 585 273 2652, ingrid_sarelius@urmc.rochester.edu.

Disclosure: The authors declare no competing financial interests.

receptors the β_2 -integrins LFA-1 and MAC-1 (8). Adhered leukocytes crawl along the EC-surface towards locations where transmigration (TEM) occurs. Leukocyte crawling was first identified in isolated cell systems (9) and later confirmed in-situ (10). Interactions between ICAM-1 and β_2 -integrins are essential for leukocyte crawling (9-10). The finding that a leukocyte's inability to crawl decreases TEM, suggests that crawling allows leukocytes to get to specific locations that accommodate TEM, and further suggests that some regions of the endothelium are better equipped to support leukocyte passage than others. While trans-cellular transmigration has been described in-vitro (11) and in-vivo (12), most agree that leukocyte TEM primarily occurs via EC-junctions (13-15). Numerous proteins associated with EC-junctions, including VE-Cadherin, CD31, CD99, JAM-1/2/3 are implicated in mediating leukocyte TEM (2,16-17). Interestingly, EC surface molecules ICAM-1 and VCAM-1 cluster at regions of leukocyte TEM, suggesting a role for these molecules in TEM as well (11, 18-19). Moreover, these molecules are localized around leukocytes that use either junctional or trans-cellular routes for emigration (11).

Tri-cellular junctions (intersection of the borders of three adjacent ECs) in particular have been suggested to serve as "portals" for leukocyte TEM, due to the discontinuity of junctional proteins, such as occludin, cadherin and ZO-1 at these sites (20). However, this does not explain trans-cellular TEM, or the finding that some junctional molecules such as VE-Cadherin can undergo rearrangement, creating de-novo gaps to accommodate leukocyte TEM (21). This report (21) implies that the preferred locations for leukocyte TEM need not pre-exist, but could be created upon receiving an appropriate signal. Whether the signal is originated in ECs or the migrating leukocytes is also not clear.

Thus the expression levels, distribution patterns and the overlap of signaling induced by all these molecules can potentially create a preferred location for leukocyte TEM.

Finally, the expression of EC junctional and surface molecules varies greatly from tissue to tissue (22), and in different locations within the vascular network (23), resulting in great variations in leukocyte-EC interactions (24). Undoubtedly the variability of junctional and surface receptors also affects the mechanisms of leukocyte recruitment. Thus, we used an intact system to explore leukocyte crawling and TEM locations in blood perfused venules in-situ. Using intravital confocal microscopy combined with immunofluorescence labeling we show that leukocytes, in their innate environment, preferentially use tri-cellular junctional regions as portals for emigration. Moreover, we demonstrate that ICAM-1 enrichment near EC-junctions likely makes these locations preferred for leukocyte TEM. EC morphology determines the number of available portals, making venular converging regions optimally equipped to support leukocyte TEM.

Materials and Methods

Animals

Male wild type (WT) C57BL6J mice (Jackson) aged 12-15 weeks were used. Animals were anesthetized with Na pentobarbital (65mg/kg, ip) and euthanized by overdose (>100 mg/kg) at the concentration of the protocols. When indicated, inflammation was induced by locally superfusing the tissue with fMLP (10 μ M in 0.01% DMSO, Sigma-Aldrich) or by treatment with mouse recombinant TNF α (0.5 μ g TNF α in 0.25ml saline, Sigma-Aldrich, intrascrotally) 4 hours prior to observations. All mice were used according to protocols approved by the University of Rochester Institutional Review Board.

Intravital microscopy

Mice were prepared for intravital microscopy and maintained throughout the experiment as described elsewhere.(25) Observations were made using an Olympus BX61WI microscope with an Olympus PlanF1 immersion objective (20×, 0.65 NA or 40×, 0.95 NA). All observed venules ranged from 30-80µm in diameter. Total leukocyte adhesion and TEM (transmigrated leukocytes in the tissue) were quantified using bright field images acquired via CCD camera (Dage MTI CD72). Leukocyte adhesion, crawling and TEM with respect to EC-junctions were quantified using confocal fluorescence images that were acquired by illuminating the tissue with a 50mW argon laser and imaging with a Nipkow disk confocal head (CSU 10, Yokogawa) attached to an intensified CCD camera (XR Mega 10, Stanford Photonics). All images were either digitally acquired or recorded to a DVD recorder (SONY DVO100MD) at 30 frames per second (fps) for offline analysis.

In situ immunofluorescence labeling

Selected venules were (separately) stained for PECAM-1, VE-Cadherin and ICAM-1 as previously described (23). Briefly, using microcannulation, venules were locally perfused with antibodies as follows: anti-PECAM-1 (ER-MP12 monoclonal antibody conjugated to Alexa 488, Serotec, 10µg/ml, 10 minutes); anti-VE-Cadherin (BV13 monoclonal antibody conjugated to Alexa 488, Ebioscience, 30µg/ml, 10 minutes); anti-ICAM-1 (YN/1.7.4, eBioscience, 50µg/ml, 15 minutes) followed by goat anti-rat secondary fluorescent polyclonal antibody (Alexa 488 anti-rat, Molecular Probes, 50 µg/ml, 15 minutes) or, alternatively, anti-ICAM-1 (YN/1.7.4 conjugated to Alexa 488, BioLegend, 30µg/ml, 10 minutes).

Unless stated differently, to observe leukocyte behavior with respect to EC-junctions, leukocytes were stained for CD11a (anti-CD11a-Alexa 488 (M17/4), Ebioscience, 3µg/mouse, i.v) in addition to the anti-PECAM-1-Alexa 488 antibody, as above. Because the EC-junctions are stationary and leukocytes are mobile, leukocytes can be easily resolved with respect to EC-junctions despite using the same fluorophore. While M/17.4 is able to block integrin function, as shown in Supplemental Figures S1 and S2, M/17.4 combined with ER-MP12 antibodies at the concentrations used in this work did not affect the specified leukocyte behavior. Anti-VE-Cadherin (BV13, 30µg/ml) antibody left the EC-junctions intact, with no visible gaps after 2hours (Figure S3).

Penetratin-ICAM-1 tail peptides

The peptides used consisted of 16 amino acids of penetratin (RQIKIWFQNRRMKWKK) followed by 13 C-terminal amino acids of mouse ICAM-1 (QRKIRIYKLQQAQ); this peptide was modified for mouse tissue from a previous report (18). The control peptide was an irrelevant sequence from rat rodopsin (CKPMSNFRFGENH). In all cases selected venules were locally perfused with the relevant peptide (100µg/ml, 15 minutes) prior to tissue stimulation with fMLP.

Analyses

Leukocyte interactions—A venular convergence was defined by measuring 40µm (an average length of venular EC (23)) in each direction from the inner convergence point for each of the inflow vessels at the convergence (see Fig 2A top panel). This 80µm length was used to quantify leukocyte adhesion (cells/80µm vessel wall) in convergences (regions 1, 1* and 2, white dotted lines, Fig 1D) and in straight regions at least 40µm away (designated region 3, not illustrated). All leukocytes that remained stationary, or did not exceed a displacement of more than 8µm (one leukocyte diameter) during 30 seconds were considered adhered. In all cases regions 1 and 1* surrounded the smaller of the two inflow vessels. For TEM, leukocytes were counted in the extravascular tissue regions 1, 1*, 2 (Fig 1D, black dotted lines) and 3 (not

illustrated) adjacent to vessels lengths where the adhesion was quantified. Regions 1, 1*, 2 for TEM were defined as follow: *Region 1* (between the two inflow vessels) was defined by projecting two lines perpendicular to the vessel walls. *Regions 1** and 2 were defined by connecting two lines that were projected perpendicular to each vessel, and that were equal in length to the diameter of the vessel they were projected from (illustrated in black). Adhesion and TEM in regions 1 and 1* were averaged and presented as region 1. In straight regions, transmigrated leukocytes were counted in the tissue within 50 μm of the vessel/80 μm length vessel segments. All TEM counts were normalized to 1000 μm^2 . To quantify leukocyte crawling and TEM routes, leukocytes and ECs were visualized as described above; each site was observed and recorded for 30-40 minutes at 30 frames per second (fps). The original movies were timelapsed to 0.33 fps for offline analysis. Leukocyte crawling was defined as a displacement of at least one average leukocyte diameter (8 μm) during 30 minutes. Only rolling leukocytes which were observed to firmly adhere and then began to crawl were analyzed. Any crawling leukocytes that crawled out of the field of view were not included in the analysis. Ccrawling distances were obtained by measuring the path length of each crawling leukocytes from the moment it began to move and until it either detached from the endothelium or underwent TEM. A leukocyte was considered to be migrating via a junctionally associated route if immediately prior to TEM, it was observed to intersect with the EC-junction, and exhibited no measurable lateral displacement as it passed through the endothelial layer. When unclear, we assigned the transmigrating pathway to “un-assg”.

EC-junctions—The number of junctions was quantified in convergences and the average area of all convergences (6000 \pm 187 μm^2 , n=11) was used as a region of interest (ROI) for comparative analysis of straight regions. Vessel diameter in each straight region was used as the width of the ROI and the length was adjusted as needed to achieve an area of 6000 μm^2 (see Fig 2A, bottom panel). All dimensions were calculated from lengths measured as 2-dimensional projections of the 3-dimensional length; this measurement has <13% projection error (10). All images were acquired as “continuous stacks” and presented as summed z-stack projections for measurement of EC-junctional length.

ICAM-1 enrichment—To determine the level of ICAM-1 enrichment, 3 independent measurements on the EC-surface were taken. ICAM-1 expression near tri-cellular junctions was measured by placing a 5 μm -diameter ROI at the edges of each EC comprising the junction, as close as possible to each outlined junction. The mean intensity of the 3 ROIs represents the ICAM-1 intensity near that junction. These measurements were taken for all tri-cellular junctions in the field of view. Similarly, two measurements of ICAM-1 intensity were taken on each side of all bi-cellular junctions, and averaged. A third measurement was taken randomly in the middle of each EC, away from all junctions. Each ROI measurement was normalized to the mean intensity of the whole EC on which it was located. Intensities that were 2 SD higher than the mean intensity of the ROIs on the EC-surface away from junctions were defined as enriched regions. Similar analyses were performed on ECs that were labeled using only the primary anti-ICAM-1 Ab (YN-1) conjugated to Alexa 488, as controls for possible clustering induced by secondary antibody. No differences were found (data not shown). For an additional control, similar analyses were performed on ECs stained for the unrelated adhesion molecule P-selectin, using primary followed by secondary Abs (similarly to principal approach for labeling of ICAM-1). This showed no P-selectin enrichment in the tri-cellular junctional regions thus further supporting our conclusion that the observed enrichment of ICAM-1 was not an artifact (Fig 6A).

Statistics

Statistical significance was assessed by one way ANOVA with Newman-Keuls Multiple Comparison Test using Graphpad Prism (V4.0). Statistical significance was set at P<0.05.

Results

Leukocyte adhesion and transmigration primarily occur in venular convergences

We have previously demonstrated increased leukocyte adhesion and TEM in converging regions of TNF α -activated venules (26). Similarly, in the present study, fMLP-induced leukocyte adhesion and TEM were significantly increased in venular convergences (*region 1*) compared to the neighboring straight regions (*region 3*, Fig 1A).

The number of adhered leukocytes in *region 1* of the convergence was significantly higher compared to *region 2* and *region 3* (7.0 ± 0.4 vs. 5.1 ± 0.4 and 4.3 ± 0.5 , leukocytes/80 μ m vessel length, respectively, $p<0.01$, Fig 1B). Likewise, leukocyte TEM in *region 1* was significantly higher compared to *regions 2 and 3* (29.75 ± 3.1 vs. 12.6 ± 1.3 and 11.3 ± 1.3 leukocytes/10000 μ m² tissue, respectively, $p<0.001$, Fig 1C). Leukocyte TEM localized to the convergence but not the straight venular region is shown in Figure 1E (and online Movie 1), and Figure 1F, which displays the origins and paths of transmigrating leukocytes. In this particular vessel leukocyte TEM is mostly localized to one side of the vessel wall (the upper part of the field of view). In different vessels TEM occurs at specific locations and can primarily occur from either side of the vessel wall or both sides simultaneously, and is likely a function of the distribution of the “active portals” for TEM. In control (unstimulated) tissue the number of adhered leukocytes was 1 to 2 leukocytes/80 μ m vessel length, and was not significantly different in all regions (data not shown). Similarly, the number of extravasated leukocytes ranged between 1 and 4 leukocytes/10000 μ m² and was not different in all regions (data not shown). In comparison to the findings for adhesion and TEM, leukocyte rolling fluxes (6.6 ± 0.5 vs. 5.2 ± 0.7 and 5.8 ± 0.6 , leukocytes/40sec for *regions 1, 2 and 3* respectively, Fig 1A) and rolling velocities (7.5 ± 0.8 vs. 8.2 ± 0.6 and 9.1 ± 0.8 μ m/sec) were not different in converging and straight venular regions. These data confirm that proinflammatory stimuli dramatically increase the number of firmly adhered and transmigrating leukocytes, and importantly, this data suggest that vessel architecture might play a role in leukocyte recruitment in-situ.

EC morphology is different in converging compared to straight venular regions

We have previously explored the differences in flow profiles in straight and converging regions (25-27), and concluded that flow is unlikely to be the main cause for increased leukocyte TEM in venular convergences. EC-morphology varies greatly in different vessels (23), thus we hypothesized that increased leukocyte TEM in venular convergences might result from local differences in EC morphology (e.g. size and shape), leading to different EC alignment and junctional arrangement compared to straight regions. Confirming our hypothesis, we found that in 30-60 μ m diameter venules, ECs in the convergence regions were significantly shorter (38.2 ± 0.8 vs 52.3 ± 1.1 μ m, $p<0.01$), and had significantly smaller surface area (593.8 ± 23.6 vs 879.9 ± 18.2 μ m², $p<0.01$) compared to straight regions (Table I). The aspect ratio (EC width/length, $1=\text{circle}$) in convergences was also significantly higher (0.46 ± 0.02 vs 0.34 ± 0.01 , $p<0.001$) compared to straight regions, indicating that ECs in convergences are less elongated. The alignment of ECs in these regions was significantly less ordered (17.8 ± 1.8 vs 10.6 ± 1.8 , degrees, major axis relative to axial direction, $p<0.01$, $n=219$ cells). This irregular alignment of smaller and variously shaped ECs has the potential to change the local junctional morphology, because here two, three or four adjacent ECs can create an EC junction. Thus we asked whether the number of tri-cellular EC junctions varies in straight versus converging venular regions. The number of tri-cellular junctions in convergences was indeed significantly higher compared to straight regions (20.7 ± 1.2 vs 12.43 ± 1.1 junctions/6000 μ m², respectively), but the total junctional length per area of vessel wall was not different (623.8 ± 54.8 vs 609.0 ± 28.3 μ m/6000 μ m² respectively, Fig 2B). In contrast, arteriolar ECs which differ from venular ECs in being significantly longer, (23)) maintain similar morphology in straight and converging regions (data not shown). Consequently, the number of tri-cellular junctions is not significantly

different in straight versus converging regions (8.2 ± 0.9 vs 7.9 ± 0.7 junctions/ $6000 \mu\text{m}^2$, respectively, Fig 2B). moreover, while the total junctional length per area of vessel wall in arterioles is similar to that in venules ($601.8 \pm 25.2 \mu\text{m}$ in arterioles vs $623.8 \pm 54.8 \mu\text{m}$ in venules at the diverging/converging regions and 616.6 ± 49.9 vs $609.0 \pm 28.3 \mu\text{m}$ in straight regions, respectively, Fig 2B), the number of tri-cellular junctions in arterioles was significantly lower ($\sim 50\%$ less) compared to venules (Fig 2B). This suggests that EC morphology can indeed affect leukocyte TEM by dictating the incidence and assembly of tri-cellular junctions.

The distribution of adhered leukocytes in convergences is different from that in straight venular regions

An important question arising from these observed morphological differences in straight and converging regions is whether they impact leukocyte recruitment and whether they could explain increased leukocyte TEM in convergences. We first asked whether the different EC-junctional arrangement in straight versus converging regions produced different distributions of adhered leukocytes with respect to EC-junctions. Representative images of leukocytes adhered at the different locations are presented in Figure 3C. Indeed, $55 \pm 1.8\%$ of firmly adhered leukocytes in convergences were associated with tri-cellular junctions, leaving $24 \pm 3.6\%$ and $20 \pm 3.0\%$ at bi-cellular and non-junctional regions respectively (Fig 3A). In contrast, in straight regions most adhered leukocytes ($58 \pm 2.3\%$) were located at bi-cellular junctions and only $21 \pm 2.8\%$ were located at tri-cellular EC-junctional regions (Fig 3A).

To determine whether locations of adhered leukocytes were a direct consequence of EC morphology (different ratio of bi- to tri-cellular junctions), we randomly generated x-y position coordinates for test “leukocytes” on the mapped EC morphology. The distribution of randomly adherent “virtual” cells was not different from that for actual leukocytes, as shown in Figure 3B. This implies that leukocyte adhesion on bi- versus tri-cellular junctions is a direct consequence of EC morphology.

Most leukocytes transmigrate via locations elsewhere from where they originally adhered

To study the behavior of adhered leukocyte prior to TEM, leukocytes and EC-junctions were fluorescently labeled with anti-CD11a and anti-PECAM-1 antibodies, respectively. Confirming previous findings (12), we show that most leukocytes ($92.2 \pm 1.6\%$, Fig 4A) in straight regions undergo intraluminal crawling. The majority ($89.6 \pm 1.7\%$, Fig 4A) of adhered leukocytes in convergences also crawled, but average crawling distance was significantly less compared to straight regions (20.1 ± 1.1 vs $32.1 \pm 1.5 \mu\text{m}$, Fig 4B). In both regions a small subset ($\leq 10\%$) of leukocytes crawled distances of up to $100 \mu\text{m}$. Leukocyte crawling velocity in convergences was $5.4 \pm 0.3 \mu\text{m}/\text{min}$, which was significantly slower than $11.2 \pm 0.5 \mu\text{m}/\text{min}$ in straight regions (velocity distribution, Fig 4C). Interestingly, in both straight and converging regions leukocyte crawling distances (real time trajectories) were not significantly different from their straight line displacement from origin (20.1 ± 1.1 vs $16.7 \pm 1.8 \mu\text{m}$, in convergences and 32.1 ± 1.5 vs $26.0 \pm 2.6 \mu\text{m}$ in straight regions, respectively), suggesting that there was some directionality in the observed crawling. Furthermore, following fMLP application most leukocytes crawled in the direction of, or perpendicular to, blood flow but not against it (Fig 4D,E), unlike in control venules, where leukocyte crawling is independent of the flow direction (10,28). Together these data strongly suggest that the locations where leukocytes initially adhere are merely a station where leukocytes pause, subsequently crawling to locations where the environment is right for TEM.

Leukocytes preferentially transmigrate at or near tri-cellular junctions

Leukocytes crawl finite distances of up to $\sim 100 \mu\text{m}$ (Fig 4) prior to either undergoing TEM or detaching from the vessel wall. While only a small fraction of crawling leukocytes eventually undergo TEM, this process is significantly more efficient in convergences compared to straight

regions (32.8 ± 6.1 vs 14.6 ± 6.2 % TEM/adhered, Fig 5B). The rest of the crawling leukocytes become more rounded and detach from the endothelium. The trajectory of a representative leukocyte that crawled towards the EC junctional region and transmigrated is shown in Figure 5D (online, Movie 2).

Because it has been suggested that leukocyte TEM occurs at tri-cellular junctions (20), we hypothesized that the higher TEM in convergences was due to the higher number of tri-cellular junctions in these regions. We show that in-situ, leukocyte TEM occurs primarily via a junctionally associated route in both straight and converging regions (91.3 ± 0.6 and 87.7 ± 1.7 %, respectively, Fig 5A). In convergences most (59.3 ± 2.1 %) leukocytes used tri-cellular junctions to undergo TEM versus 45.8 ± 4.1 % using bi-cellular junctions. In straight regions, equal fractions of leukocytes underwent TEM via tri-cellular and bi-cellular junctions (45.1 ± 4.1 and 45.0 ± 5.0 %, respectively, Fig 5C), despite that significantly more adhered leukocytes were originally adhered at bi-cellular compared to tri-cellular junctions (58.2 ± 2.2 vs 28.4 ± 2.1 %, Fig 3A). This again implies a clear preference towards tri-cellular junctional regions for TEM.

Consistent with the idea that TEM preferentially occurs at tri-cellular junctional regions, we also found that in arterioles (where both leukocyte adhesion and transmigration are rare events) the number of tri-cellular junctions was not significantly different in straight versus converging regions (Fig 2B), but was significantly lower (~ 50 % less) compared to venules. Together these data suggest that EC morphology and alignment, and in particular the number of tri-cellular junctions, play a key role in determining preferred regions for leukocyte transmigration.

Pro-inflammatory activation redistributes ICAM-1 towards the edges of ECs that form tri-cellular junctions

The distribution of ICAM-1 on ECs is not uniform, and under appropriate conditions undergoes redistribution to more localized regions within individual ECs (23). Furthermore, ICAM-1 clustering occurs around transmigrating leukocytes (11,19,29), suggesting that regions surrounding tri-cellular junctions could also be enriched in ICAM-1. If true this would explain why these junctional regions are preferred locations for TEM.

We show that 50 minutes following fMPL application, the expression of ICAM-1 on the EC-surface significantly increased (Figure S4A). Likewise, ICAM-1 was enriched near EC-junctions (Fig 6A,B). Representative images in Fig 6A demonstrate enrichment of ICAM-1 (second panel from the top), near tri-cellular junctions in venules in fMLP treated tissue (middle), but not under control conditions (upper panel). ICAM-1 enrichment was also observed with TNF α treatment, which is known to directly activate ECs (third panel from the top), but not P-selectin (bottom). P-selectin (green) exhibits a typical punctate distribution on EC surface (as previously determined, (27, 30)), but no preferential localization to the EC-junctions (red). Importantly, approximately 43% of tri-cellular junctions were associated with enriched ICAM-1 versus only 23% of bi-cellular junctions, directly supporting our hypothesis that ICAM-1 at least in part contributes to making the tri-cellular endothelial junctions a preferred location for leukocyte TEM. This enrichment occurred in both converging and straight regions (data not shown). The finding that not all tri-cellular junctions are enriched in ICAM-1 suggests that not all of them will equally support TEM. Supporting this, we determined that ~ 40 % of all crawling leukocytes that transmigrated, crossed at least one tri-cellular junction on their way to a transmigratory portal. The trajectory of a typical crawling leukocyte crossing two tri-cellular junctions is shown in Figure 6E (online, Movie 3). Furthermore, we found that leukocyte crawling was slowest across tri-cellular junctions (4.2 ± 0.3 , straight and $4.1 \pm 0.3 \mu\text{m}/\text{min}$, converging regions, Fig 6C); velocity across bi-cellular junctions was also significantly slower than at non-junctional regions (7.6 ± 0.6 vs $11.1 \pm 0.7 \mu\text{m}/\text{min}$, in straight and 7.1 ± 0.4 vs $10.4 \pm 0.6 \mu\text{m}/\text{min}$, in converging regions, respectively, Fig 6C). Moreover, individual leukocytes that crawled for longer distances ($>40 \mu\text{m}$), and

crossed at least two tri-cellular junctions, predictably slowed down near the EC-junction and sped up on the EC surface (Fig 6D). A representative velocity trace of a leukocyte in relation to EC-junctions and its crawling trajectory are shown in Figure 6D (bottom). The leukocyte slowed down near tri-cellular junctions, consistent with evidence for ICAM-1 enrichment in these regions (Figure 6A,B). Crawling velocity across EC-cellular junctions was not different in straight vs. converging regions (Fig 6C) suggesting that the differences in leukocyte crawling behavior in both regions are indeed relatable to local ICAM-1 distribution.

ICAM-1 signaling is required for junctional rearrangement allowing leukocyte passage

ICAM-1 engagement leads to phosphorylation of junctional proteins, such as VE-Cadherin (31), likely contributing to its redistribution away from junctions during TEM (21). We observed redistribution of VE-Cadherin and formation of gaps at the locations of leukocyte TEM in-situ (as described in monolayers (21)) following fMLP treatment of the tissue, but not in untreated venules (Fig 7A, and representative images 7C, middle and upper panels). Importantly, gap formation was significantly attenuated by treatment with the ICAM-1 tail peptide that blocks ICAM-1 signaling (18) (Fig 7A and representative image 7C, bottom panel), consistent with the hypothesis that high ICAM-1 density around EC-junctions is important for VE-Cadherin rearrangement. Approximately 70% of all observed gaps were formed in association with tri-cellular junctions (Fig 7B), confirming that these are preferred TEM locations. Despite the overall lower number of gaps formed following treatment with the ICAM-1 tail peptide, the same ~ 70% were still seen in association with the tri-cellular junctions (Fig 7B).

We also tested the effect of ICAM-1 tail peptide on leukocyte behavior, and compared this with the effect of a monoclonal antibody that blocks luminal interactions of leukocytes with ICAM-1. As predicted from isolated cell systems (18), treatment with the ICAM-1 tail peptide did not significantly alter the ability of leukocytes to adhere or crawl on the endothelium (thus presumably did not affect their ability to reach the right location for TEM) but reduced leukocyte TEM by 71% (Fig 7D), indicating that the inability to open EC-junctions is the cause of impaired leukocyte TEM. The direction of crawling, and leukocyte crawling velocity also remained unchanged (Figs 7E,G). Interestingly, treatment with the ICAM-1 tail peptide significantly increased leukocyte crawling distances (41.4 ± 2.4 vs. $28.9 \pm 2.7 \mu\text{m}$ in untreated venules, Fig 7F), implying that reduced TEM was due to the inability of leukocytes to find the portal locations. Furthermore, one of every four leukocytes that were observed undergoing TEM following blockade of the ICAM-1 tail had difficulty in disengaging from the endothelium as it traversed the vessel wall. Antibody blockade of ICAM-1, as expected (32), significantly decreased leukocyte adhesion (42%), abrogated leukocyte crawling (84%), and resulted in a 68% decrease in leukocyte TEM (Fig 7D). Interestingly, the residual crawling was significantly slower than that in untreated venules (6.5 ± 0.9 vs. $10.5 \pm 0.8 \mu\text{m}/\text{min}$ Fig 7G), and the direction of crawling was more random (same fraction in all directions, Fig 7E), confirming a role for ICAM-1 in directing leukocyte crawling. Treatment with either a non-specific antibody or a control peptide had no significant effect on leukocyte adhesion and TEM, and did not prevent the formation of gaps in VE-Cadherin (data not shown). Together these findings suggest a dual role for ICAM-1 in mediating leukocyte TEM: signaling to leukocytes the location of a portal for TEM, and preparation of EC-junctions to accommodate leukocyte passage.

Discussion

Leukocyte TEM occurs primarily at EC-junctions (12,21,33), but recent studies suggest that changes in EC morphology, and consequently junctional arrangement, or disruption of β_2 -integrin-ICAM-1 interactions, can lead to transcellular migration (12,18). Thus here we asked

whether differences in EC morphology in straight and converging venular regions affect leukocyte trafficking and TEM in-situ. We showed that leukocytes, in their innate environment, preferentially use tri-cellular junctional regions as “portals” for TEM. Our data suggest that the “portals” are junctions that are surrounded by enriched regions of ICAM-1. These enriched ICAM-1 regions mark the location of a nearby portal, as well as preparing the EC-junctions to accommodate leukocyte passage. Thus, discontinuities in junctional molecules need not pre-exist, but can be initiated by approaching leukocytes via ICAM-1-mediated signaling. Supporting our findings, others have found no evidence for pre-existing discontinuities of the endothelial barrier at tri-cellular junctions in retinal wholemounts, but observed loss of tight junction proteins during leukocyte TEM (34). While we can not unequivocally demonstrate that all leukocytes transmigrating via these portals were taking a junctional route (vs a paracellular route in very close apposition to the actual junction), our findings that the ICAM-1 tail peptide blocked leukocyte TEM and VE-Cadherin rearrangement at the EC junctions, together with the findings that ICAM-1 mediated signaling directly affects VE-Cadherin phosphorylation and mobility (30), strongly argues that route taken is indeed junctional.

Rearrangement of junctional molecules such as VE-Cadherin, and formation of transient gaps during leukocyte TEM has been demonstrated in-vitro (21,35-36). We confirmed these findings in-situ, and, further, showed that signaling mediated via the ICAM-1 cytosolic tail is essential for the formation of observed gaps in VE-Cadherin. As the ICAM-1 tail is a potential binding target for Src (37), the likely signaling mechanism for the disassembly of the homologous VE-Cadherin interactions is the activation of proteins Src- and Pyk2 upon engagement of ICAM-1, leading to phosphorylation of VE-Cadherin (31). However, the ability of leukocytes to exert force on EC contacts during TEM (38) could also contribute to the formation of these gaps, and cannot be ruled out.

We add another dimension to the complexity of recruitment by showing that the arrangement of EC-junctions in different venular regions greatly contributes to leukocyte recruitment and TEM. ECs in venular convergences are significantly smaller, more rounded and aligned in a more random fashion than ECs in straight regions (Table 1). This arrangement produces more tri-cellular junctions in convergences, apparently making convergences optimally equipped to support TEM. In previous work we also showed that in venular convergences the two inlet vessels are predicted to create a region of low velocity, increasing leukocyte adhesion probability (26), as was indeed demonstrated in Figure 1B. Increased leukocyte adhesion together with a higher number of tri-cellular junctions in venular convergences, resulted in 2.6-fold higher leukocyte TEM compared to straight regions. Thus, while fluid shear likely contributes to leukocyte accumulation in convergences, it is unlikely to affect leukocyte TEM directly. This is because not only the absolute number (higher as a result of more adhered cells in the region), but also TEM efficiency (% TEM/all adhered cells) was significantly higher in convergences (Fig 5B). Similarly we ruled out the differential expression of adhesion molecules as key contributors for increased TEM, as the expression of ICAM-1 (Fig S4B) and E-selectin (unpublished) is not different in straight versus converging regions, confirming local EC morphology as a prime candidate.

Previous analysis of leukocyte adhesion in-vivo (10), and work in monolayers (39), showed that due to the EC morphology, most adhered leukocytes overlap EC-junctions. We have extended these findings to show that differences in leukocyte adhesion distribution with respect to junctional type in convergences versus straight regions are solely due to differences in EC size, shape and alignment, producing a higher ratio of tri-cellular to bi-cellular junctions in venular convergences.

Leukocyte crawling is presumably a tool to get adhered leukocytes to the nearest EC junction, where TEM occurs. Confirming previous observations (10,12), we showed that nearly 90% of

leukocytes undergo intraluminal crawling (Fig 4). This suggests that the initial location of leukocyte adhesion is simply a way station where leukocytes pause before crawling to a “portal” to undergo TEM. Leukocyte crawling, in control venules and monolayers (28,39) or in MIP-2 stimulated venules (12) is random (independent of blood flow). However, in our study, leukocyte crawling in the presence of fMLP was parallel or perpendicular to blood flow, but very rarely against it, suggesting some degree of directionality. The finding that blockade of the luminal portion of the ICAM-1 molecule, but not blockade of the cytoplasmic tail, resulted in loss of the observed directionality (Fig 7E), argues that ICAM-1 might play a role in directing leukocyte crawling.

We showed that 50 minutes after fMLP application ICAM-1 expression was significantly increased (Fig S4A) compared to control conditions, indicating endothelial activation. The fMLP evoked response in this time frame is surprising as fMLP is considered to be a leukocyte activator, and there is very little evidence for its ability to affect ECs. Whether the increase in ICAM-1 expression was directly induced by fMLP treatment or whether it was a consequence of fMLP-induced leukocyte activation and adhesion is not clear and will require new studies. Importantly, upon exposure of the tissue to fMLP, otherwise homogeneously expressed ICAM-1 on individual ECs became enriched near EC-junctions (primarily tri-cellular, Fig 6A,B). The presence of ICAM-1-enriched regions near tri-cellular junctions could explain the shorter crawling distances that leukocytes exhibit in venular convergences, as well as their lower crawling velocities (Fig 4D).

In our preparation fMLP-induced TEM occurred mainly at or very close to EC-junctions. Our results differ from those previously reported (40), possibly due to the route of fMLP administration or the different tissue that was investigated. Intriguingly, leukocytes that originally adhered at bi- or tri-cellular junctions were often observed to crawl away and either detach from the endothelium or transmigrate elsewhere. This argues that initial adhesion doesn't determine whether the leukocyte will undergo TEM, or affect the route it will use, although this requires future studies. It also suggests that not all EC-junctions are the same; some EC-junctions can act as “portals” for leukocyte TEM and some apparently cannot. Our study implicates ICAM-1 in making some EC-junctions act as portals for TEM.

Many molecules make up EC-junctions, and most have been implicated in leukocyte TEM (14,16,41). Importantly, the nature of endothelial cell-cell contacts varies with the need to regulate vessel barrier function. For example, arterioles have a significantly higher number of tight junctions compared to venules (42), and are significantly less permeable (43). Likewise, there are differences in expression and subcellular localization of junctional adhesion molecules (JAM) (22). In the current work we suggest that the junctions that could act as portals for TEM are those junctions that are surrounded by high ICAM-1 expression, but an alternative/additional explanation could be that active portals have a different assembly or different array of junctional proteins compared to elsewhere. The local microanatomy of these junctions might also be different.

As mentioned above, not all junctions are used by leukocytes for TEM. In fact, only a small portion of the junctions act as active portals, and often the same junctional region (bi- or tri-cellular) is used by multiple leukocytes. Supporting the idea that portals are EC-junctions that are enriched in ICAM-1, only ~43% of all tri- and 23% of all bi-cellular junctions became enriched in ICAM-1, correlating with the percentages of leukocytes undergoing TEM in these regions. Moreover, we showed that gaps in VE-Cadherin staining were primarily formed at tri-cellular junctions (Fig 7), and were mediated via ICAM-1 signaling, again suggesting that the observed leukocyte behavior is directly connected to ICAM-1 enriched regions.

Some regions within the venular wall express lower levels of key extracellular matrix proteins comprising the basal lamina than other regions in the same vessel (44). These regions are also associated with gaps between the pericytes and are preferentially used by migrating leukocytes (44). We speculate that localization of these regions with EC-junctions could also make these locations optimal for leukocyte TEM.

In summary, we show that leukocytes in their innate environment preferentially target tri-cellular EC junctions to traverse the vessel wall. We show that EC morphology plays an important role in determining these portals, making venular converging regions optimally equipped to support leukocyte TEM. Moreover, in exploring the nature of the active portals, we suggest that enrichment of ICAM-1 surrounding some EC-junctions makes these locations preferred for TEM, by signaling to leukocytes the location of the portal, and further by mediating rearrangement of junctional molecules at these locations.

Supplementary Material

Refer to Web version on PubMed Central for supplementary material.

Acknowledgments

We thank J.M. Kuebel for expert technical assistance and Hen Drori for thoughtful discussion.

This work was supported by NIH RO1 HL75186, NIH PO1 HL18208

References

1. Ley K, Laudanna C, Cybulsky MI, Nourshargh S. Getting to the site of inflammation: the leukocyte adhesion cascade updated. *Nat Rev Immunol* 2007;7:678–689. [PubMed: 17717539]
2. Muller WA. Leukocyte-endothelial-cell interactions in leukocyte transmigration and the inflammatory response. *Trends Immunol* 2003;24:327–334. [PubMed: 12810109]
3. Nourshargh S, Marelli-Berg FM. Transmigration through venular walls: a key regulator of leukocyte phenotype and function. *Trends Immunol* 2005;26:157–165. [PubMed: 15745858]
4. Alcaide P, Auerbach S, Luscinskas FW. Neutrophil recruitment under shear flow: it's all about endothelial cell rings and gaps. *Microcirculation* 2009;16:43–57. [PubMed: 18720226]
5. Kansas GS. Selectins and their ligands: current concepts and controversies. *Blood* 1996;88:3259–3287. [PubMed: 8896391]
6. Ley K, Allietta M, Bullard DC, Morgan S. Importance of E-selectin for firm leukocyte adhesion in vivo. *Circ Res* 1998;83:287–294. [PubMed: 9710121]
7. McEver RP, Cummings RD. Role of PSGL-1 binding to selectins in leukocyte recruitment. *J Clin Invest* 1997;100:S97–103. [PubMed: 9413410]
8. Steeber DA, Tang ML, Green NE, Zhang XQ, Sloane JE, Tedder TF. Leukocyte entry into sites of inflammation requires overlapping interactions between the L-selectin and ICAM-1 pathways. *J Immunol* 1999;163:2176–2186. [PubMed: 10438959]
9. Luu NT, Rainger GE, Nash GB. Kinetics of the different steps during neutrophil migration through cultured endothelial monolayers treated with tumour necrosis factor-alpha. *J Vasc Res* 1999;36:477–485. [PubMed: 10629423]
10. Wojciechowski JC, Sarelius IH. Preferential binding of leukocytes to the endothelial junction region in venules in situ. *Microcirculation* 2005;12:349–359. [PubMed: 16020081]
11. Carman CV, Springer TA. A transmigratory cup in leukocyte diapedesis both through individual vascular endothelial cells and between them. *J Cell Biol* 2004;167:377–388. [PubMed: 15504916]
12. Phillipson M, Heit B, Colarusso P, Liu L, Ballantyne CM, Kubes P. Intraluminal crawling of neutrophils to emigration sites: a molecularly distinct process from adhesion in the recruitment cascade. *J Exp Med* 2006;203:2569–2575. [PubMed: 17116736]

13. Luscinskas FW, Ma S, Nusrat A, Parkos CA, Shaw SK. Leukocyte transendothelial migration: a junctional affair. *Semin Immunol* 2002;14:105–113. [PubMed: 11978082]
14. Nyqvist D, Giampietro C, Dejana E. Deciphering the functional role of endothelial junctions by using in vivo models. *EMBO Rep* 2008;9:742–747. [PubMed: 18600233]
15. Johnson-Leger C, Aurrand-Lions M, Imhof BA. The parting of the endothelium: miracle, or simply a junctional affair? *J Cell Sci* 2000;113(Pt 6):921–933. [PubMed: 10683141]
16. Nourshargh S, Krombach F, Dejana E. The role of JAM-A and PECAM-1 in modulating leukocyte infiltration in inflamed and ischemic tissues. *J Leukoc Biol* 2006;80:714–718. [PubMed: 16857733]
17. Liao F, Ali J, Greene T, Muller WA. Soluble domain 1 of platelet-endothelial cell adhesion molecule (PECAM) is sufficient to block transendothelial migration in vitro and in vivo. *J Exp Med* 1997;185:1349–1357. [PubMed: 9104821]
18. Yang L, Froio RM, Sciuto TE, Dvorak AM, Alon R, Luscinskas FW. ICAM-1 regulates neutrophil adhesion and transcellular migration of TNF-alpha-activated vascular endothelium under flow. *Blood* 2005;106:584–592. [PubMed: 15811956]
19. Barreiro O, Zamai M, Yanez-Mo M, Tejera E, Lopez-Romero P, Monk PN, Gratton E, Caiolfa VR, Sanchez-Madrid F. Endothelial adhesion receptors are recruited to adherent leukocytes by inclusion in preformed tetraspanin nanoplateforms. *J Cell Biol* 2008;183:527–542. [PubMed: 18955551]
20. Burns AR, Walker DC, Brown ES, Thurmon LT, Bowden RA, Keese CR, Simon SI, Entman ML, Smith CW. Neutrophil transendothelial migration is independent of tight junctions and occurs preferentially at tricellular corners. *J Immunol* 1997;159:2893–2903. [PubMed: 9300713]
21. Shaw SK, Bamba PS, Perkins BN, Luscinskas FW. Real-time imaging of vascular endothelial-cadherin during leukocyte transmigration across endothelium. *J Immunol* 2001;167:2323–2330. [PubMed: 11490021]
22. Aurrand-Lions M, Johnson-Leger C, Wong C, Du Pasquier L, Imhof BA. Heterogeneity of endothelial junctions is reflected by differential expression and specific subcellular localization of the three JAM family members. *Blood* 2001;98:3699–3707. [PubMed: 11739175]
23. Sumagin R, Sarelius IH. TNF-alpha activation of arterioles and venules alters distribution and levels of ICAM-1 and affects leukocyte-endothelial cell interactions. *Am J Physiol Heart Circ Physiol* 2006;291:H2116–2125. [PubMed: 16766643]
24. Lamkin-Kennard KA, Chuang JY, Kim MB, Sarelius IH, King MR. The distribution of rolling neutrophils in venular convergences. *Biorheology* 2005;42:363–383. [PubMed: 16308467]
25. Kim MB, Sarelius IH. Distributions of wall shear stress in venular convergences of mouse cremaster muscle. *Microcirculation* 2003;10:167–178. [PubMed: 12700585]
26. Sumagin R, Lamkin-Kennard KA, Sarelius IH. A Separate Role for ICAM-1 and Fluid Shear in Regulating Leukocyte Interactions with Straight Regions of Venular Wall and Venular Convergences. *Microcirculation* 2009:1–13.
27. Kim MB, Sarelius IH. Role of shear forces and adhesion molecule distribution on P-selectin-mediated leukocyte rolling in postcapillary venules. *Am J Physiol Heart Circ Physiol* 2004;287:H2705–2711. [PubMed: 15331369]
28. Auffray C, Fogg D, Garfa M, Elain G, Join-Lambert O, Kayal S, Sarnacki S, Cumano A, Lauvau G, Geissmann F. Monitoring of blood vessels and tissues by a population of monocytes with patrolling behavior. *Science* 2007;317:666–670. [PubMed: 17673663]
29. Millan J, Hewlett L, Glyn M, Toomre D, Clark P, Ridley AJ. Lymphocyte transcellular migration occurs through recruitment of endothelial ICAM-1 to caveola- and F-actin-rich domains. *Nat Cell Biol* 2006;8:113–123. [PubMed: 16429128]
30. Hattori R, Hamilton KK, Fugate RD, McEver RP, Sims PJ. Stimulated secretion of endothelial von Willebrand factor is accompanied by rapid redistribution to the cell surface of the intracellular granule membrane protein GMP-140. *J Biol Chem* 1989;264:7768–7771. [PubMed: 2470733]
31. Allingham MJ, van Buul JD, Burrige K. ICAM-1-mediated, Src- and Pyk2-dependent vascular endothelial cadherin tyrosine phosphorylation is required for leukocyte transendothelial migration. *J Immunol* 2007;179:4053–4064. [PubMed: 17785844]
32. Sumagin R, Sarelius IH. A role for ICAM-1 in maintenance of leukocyte-endothelial cell rolling interactions in inflamed arterioles. *Am J Physiol Heart Circ Physiol* 2007;293:H2786–2798. [PubMed: 17704289]

33. Muller WA. Migration of leukocytes across endothelial junctions: some concepts and controversies. *Microcirculation* 2001;8:181–193. [PubMed: 11498781]
34. Xu H, Dawson R, Crane IJ, Liversidge J. Leukocyte diapedesis in vivo induces transient loss of tight junction protein at the blood-retina barrier. *Invest Ophthalmol Vis Sci* 2005;46:2487–2494. [PubMed: 15980240]
35. Corada M, Mariotti M, Thurston G, Smith K, Kunkel R, Brockhaus M, Lampugnani MG, Martin-Padura I, Stoppacciaro A, Ruco L, McDonald DM, Ward PA, Dejana E. Vascular endothelial-cadherin is an important determinant of microvascular integrity in vivo. *Proc Natl Acad Sci U S A* 1999;96:9815–9820. [PubMed: 10449777]
36. Alcaide P, Newton G, Auerbach S, Sehrawat S, Mayadas TN, Golan DE, Yacono P, Vincent P, Kowalczyk A, Luscinskas FW. p120-Catenin regulates leukocyte transmigration through an effect on VE-cadherin phosphorylation. *Blood* 2008;112:2770–2779. [PubMed: 18641366]
37. Sparks AB, Rider JE, Hoffman NG, Fowlkes DM, Quillam LA, Kay BK. Distinct ligand preferences of Src homology 3 domains from Src, Yes, Abl, Cortactin, p53bp2, PLCgamma, Crk, and Grb2. *Proc Natl Acad Sci U S A* 1996;93:1540–1544. [PubMed: 8643668]
38. Rabadzey A, Alcaide P, Luscinskas FW, Ladoux B. Mechanical forces induced by the transendothelial migration of human neutrophils. *Biophys J* 2008;95:1428–1438. [PubMed: 18390614]
39. Schenkel AR, Mamdouh Z, Muller WA. Locomotion of monocytes on endothelium is a critical step during extravasation. *Nat Immunol* 2004;5:393–400. [PubMed: 15021878]
40. Feng D, Nagy JA, Pyne K, Dvorak HF, Dvorak AM. Neutrophils emigrate from venules by a transendothelial cell pathway in response to FMLP. *J Exp Med* 1998;187:903–915. [PubMed: 9500793]
41. Liu Y, Shaw SK, Ma S, Yang L, Luscinskas FW, Parkos CA. Regulation of leukocyte transmigration: cell surface interactions and signaling events. *J Immunol* 2004;172:7–13. [PubMed: 14688302]
42. Simionescu M, Simionescu N, Palade GE. Segmental differentiations of cell junctions in the vascular endothelium. *The microvasculature. J Cell Biol* 1975;67:863–885. [PubMed: 1202025]
43. Sumagin R, Lomakina E, Sarelius IH. Leukocyte-endothelial cell interactions are linked to vascular permeability via ICAM-1-mediated signaling. *Am J Physiol Heart Circ Physiol* 2008;295:H969–H977. [PubMed: 18641276]
44. Wang S, Voisin MB, Larbi KY, Dangerfield J, Scheiermann C, Tran M, Maxwell PH, Sorokin L, Nourshargh S. Venular basement membranes contain specific matrix protein low expression regions that act as exit points for emigrating neutrophils. *J Exp Med* 2006;203:1519–1532. [PubMed: 16754715]

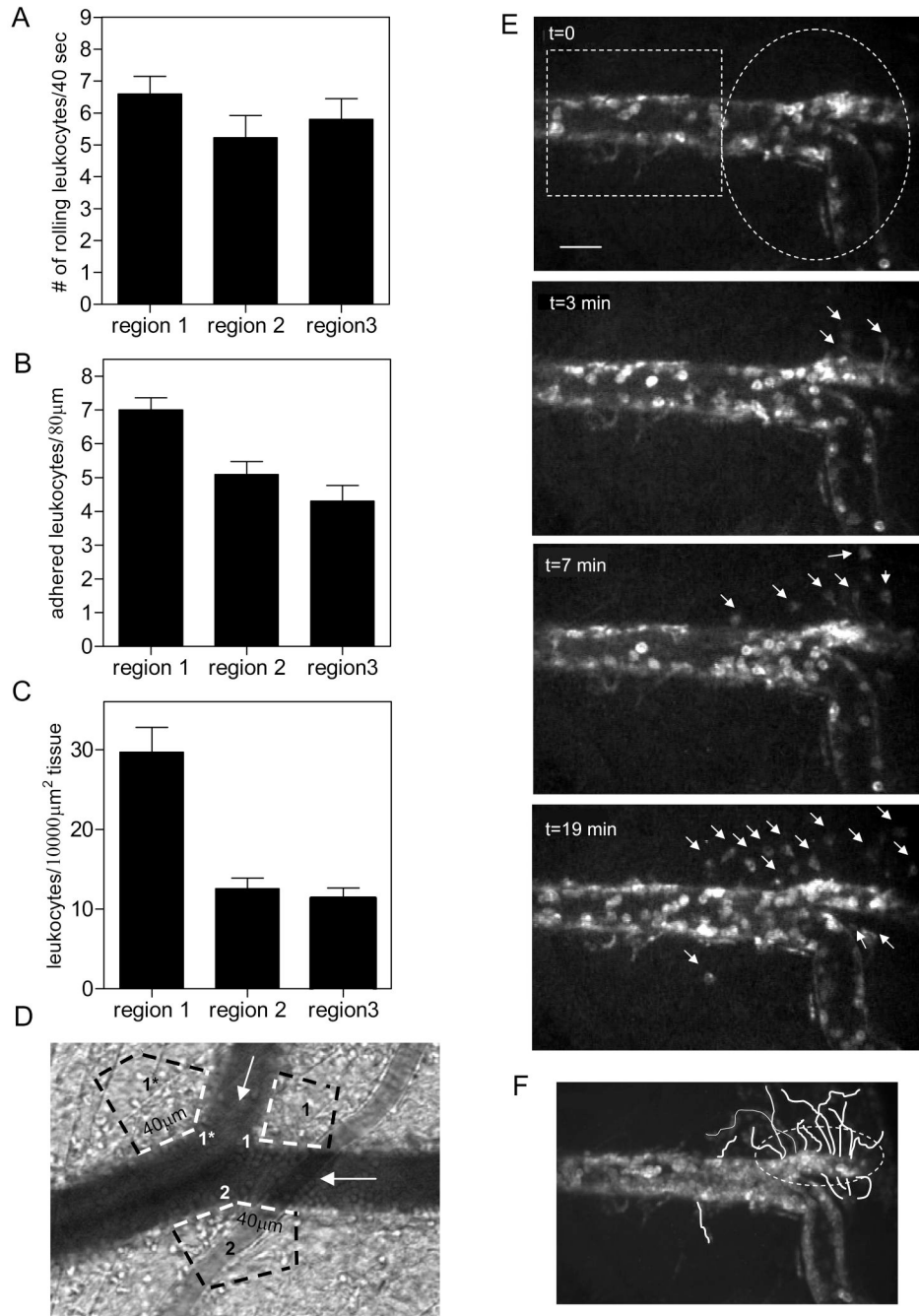


Figure 1. Leukocyte adhesion and transmigration occur primarily in venular convergences

The intact tissue was stimulated by superfusion of fMLP (10 μ M, for 10 minutes). All data were collected 40 minutes after the completion of fMLP application. Leukocyte rolling (A) adhesion (B) and TEM (C) were quantified in venular convergences (*regions 1 and 2*) and compared to straight regions (*region 3*). For adhesion and TEM (panels B and C) each data point in region 1 represents an average of leukocytes on both sides of the inflow venule (regions 1 and 1*, Fig1C). Regions 1, 1*, 2 and 3 were defined as described in the Methods section. All TEM counts were normalized to 10000 μ m². (D) Image of a representative venular convergence, where leukocyte adhesion and TEM (white and black dotted lines respectively) were quantified in regions 1, 1* and 2. To quantify leukocyte adhesion and TEM in the straight region (region

3) the field of view had to be moved away from the convergence, thus it is not illustrated. The white arrows show the direction of flow. (E) Sequence of images over 20 minutes showing leukocyte TEM in the converging region (white ellipse) vs straight venular region (white rectangle). The bar is 25 μ m. (F) Time lapsed images were summed to display the origin and path of migrating leukocytes. Both leukocyte adhesion and leukocyte TEM are significantly enhanced in the regions of venular convergences. For all groups bars are mean+SE, n=4 mice, 8 venules. ** Significantly different from other groups (p<0.01)

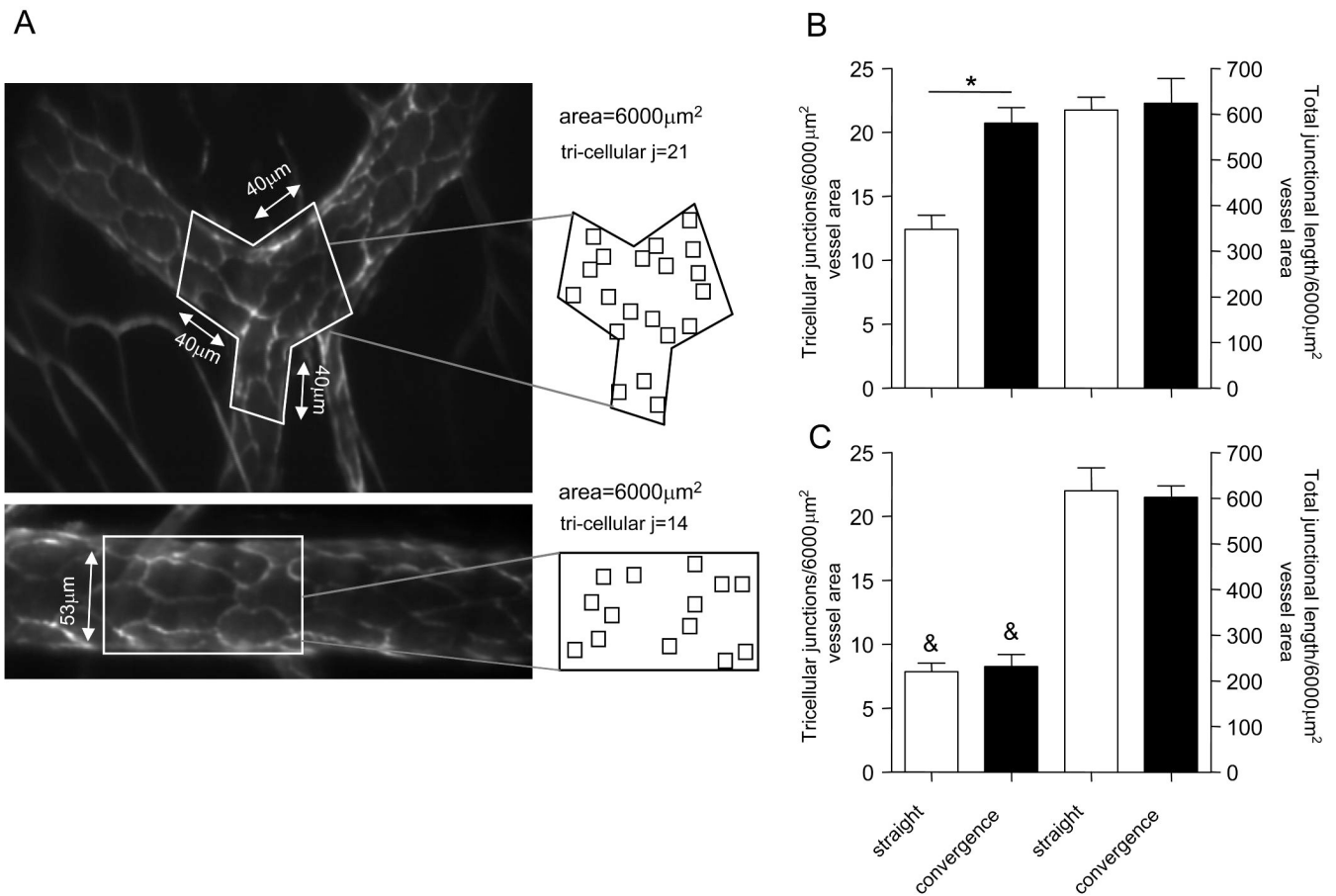


Figure 2. The number of tri-cellular junctions in venular convergences is significantly higher than in straight regions

(A) A representative image of a venular convergence and corresponding straight region (as defined in METHODS section), which were lumenally perfused with fluorescently tagged anti-PECAM-1 antibody (10 $\mu\text{g}/\text{ml}$) to visualize EC arrangement. Outlined in white are the regions (6000 μm^2) where the number of tri-cellular junctions and the total junctional length were quantified. All analyses were performed on real time recordings of each vessel where the focal plane was brought up or down as necessary, in order to focus on the specific, analyzed part of the vessel wall. The squares within the projections outline the tri-cellular junctions to demonstrate the apparent higher number of these junctions in venular convergences. (B and C) Quantification of tri-cellular junctions in straight and converging/diverging regions of sampled **venules** (B) and **arterioles** (C) respectively. For all groups bars are mean+SE, n=3-4 mice, 11 straight and converging regions. * Significantly different from each other ($p<0.05$), & Significantly different from same region in venules (Fig 2B, $p<0.05$).

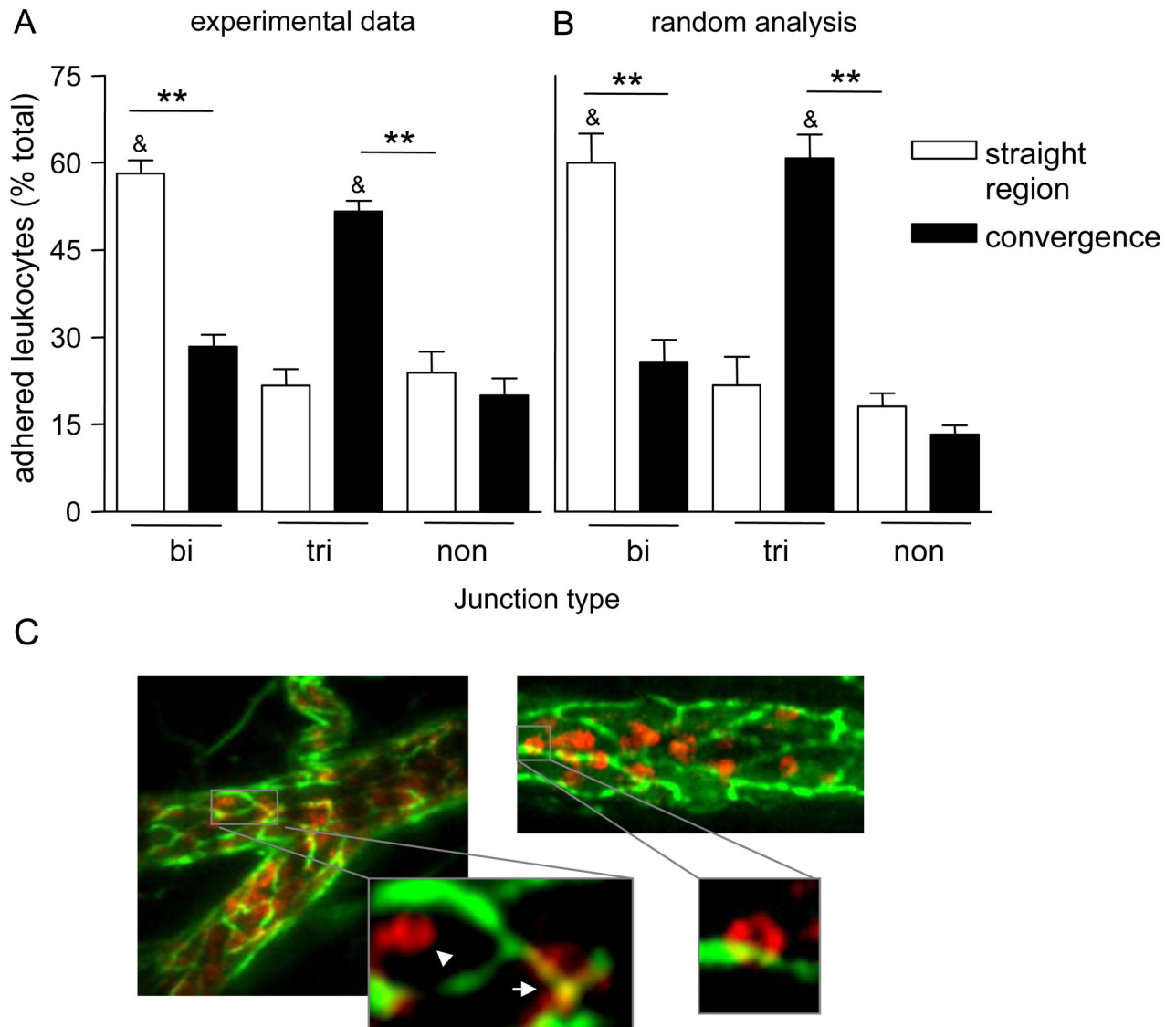


Figure 3. The distribution of adhered leukocytes is a direct consequence of the junctional arrangement

To visualize EC-junctions and circulating leukocytes, venules were locally perfused with anti-PECAM-1 conjugated to Alexa 488 (10 μ g/ml) followed by intravenous injection of anti-CD11a conjugated to Alexa 488 (3 μ g/ml) antibodies. (A) The number of firmly adhered leukocytes at bi-cellular (bi) and tri-cellular (tri) junctions, as well as on the non-junctional regions (non) were quantified. The number of adhered leukocytes at each location is presented as % of the total population. (B) Simulated leukocytes (circles with 8 μ m diameter) were positioned using randomly generated coordinates within the images of PECAM-1 stained venules that were previously obtained and used to quantify leukocyte adhesion as shown in (A). Similarly to (A), the number of leukocytes that was found at each of the junctional locations was quantified. For all groups bars are mean+SE, n=4 mice, 11 straight and converging regions. ** Significantly different from each other (p<0.01). & Significantly different from others in same group (p<0.01). (C) For illustrative purposes the endothelium of a blood perfused venule was stained for PECAM-1 (anti-PECAM-1 conjugated to Alexa 488, 10 μ g/ml) and leukocytes were stained for CD11a (Phycoerythrin anti-CD11a, 3 μ g/mouse, red). Representative images

(which are z-stack projections of multiple focal planes) depict adhered leukocytes in straight and converging venular regions. The zoom-in images are a single slice of a Z-stack, and show firmly adhered leukocytes at the non-junctional (arrow head), tri-cellular (short arrow) and bi-cellular junctional regions, thus the colocalizing yellow signal. Due to the higher abundance of tri-cellular junctions in convergences (compared to straight regions), most adhered leukocytes in these regions are found on the tri-cellular junctions.

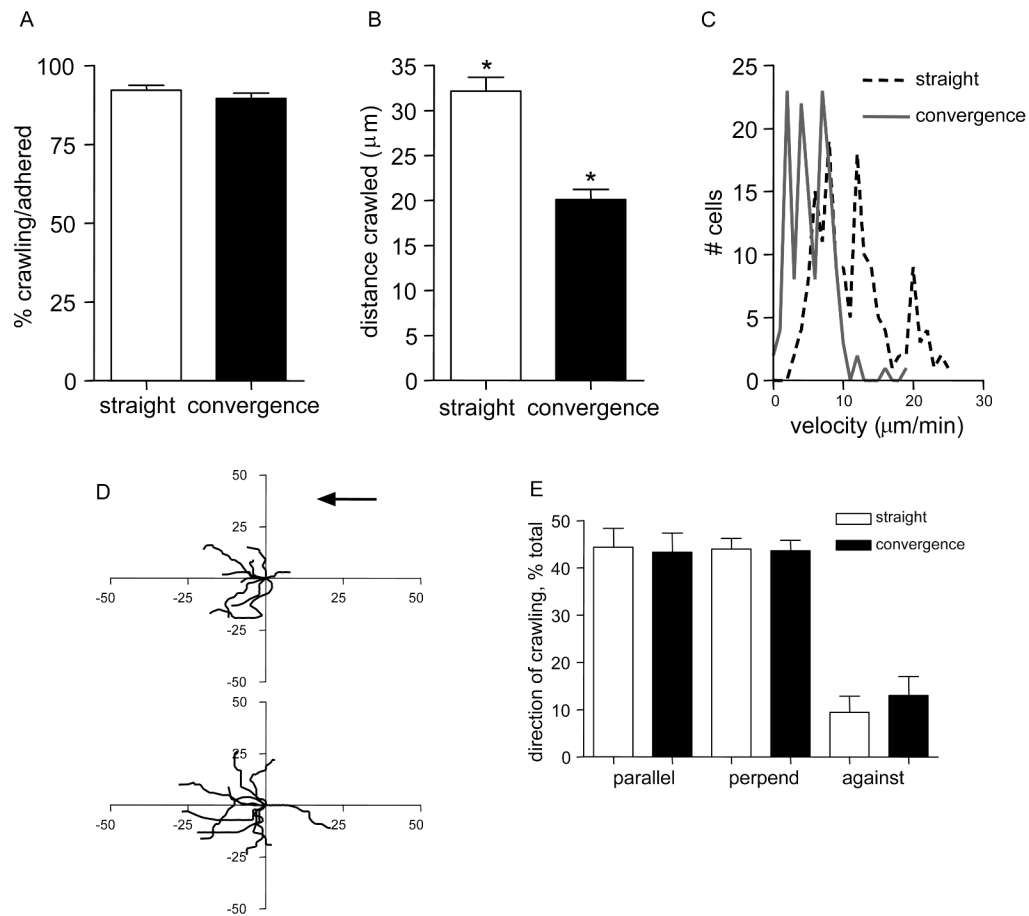


Figure 4. Crawling distances and crawling velocities are significantly less in convergences compared to straight regions

EC junctions and interacting leukocytes were immunofluorescently labeled using anti-PECAM-1 conjugated to Alexa 488 (10µg/ml, local perfusion) and anti-CD11a conjugated to Alexa 488 (3µg/ml, i.v). Time lapsed microscopy ($\times 90$) was used to track crawling leukocytes in straight and in converging regions. (A) The fraction of adhered leukocytes that crawled in each region was not different. (B,C) Leukocyte displacement (B), and the mean velocity (C, presented as frequency distribution plot) were less in convergences compared to straight regions. (D) Representative leukocyte crawling trajectories (n=11) from two straight (upper panel) and two converging (lower panel) venular regions. All starting positions were aligned to the same origin. Black arrow indicates flow direction. Axes, distance in micrometers. (E) The direction of leukocyte crawling with respect to blood flow. Directions were defined as follows: Parallel to blood flow (within ± 45 degrees (parallel)); perpendicular to blood flow (between ± 45 and 90 degrees (perpend)); past the origin in the negative direction of the blood flow (against). For all groups in panels A-C and E, n=188 leukocytes in 9 straight and n=148 leukocytes in 7 converging regions in 5 mice were tracked. Bars are mean+SE. * Significantly different from each other ($p < 0.05$).

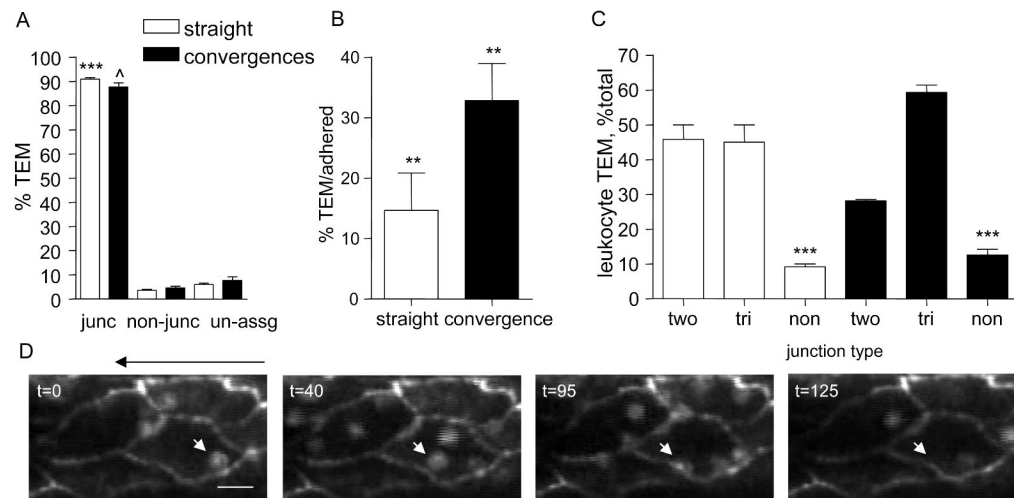


Figure 5. Leukocytes preferentially transmigrate at tri-cellular junctions

EC-junctions and interacting leukocytes were immunofluorescently labeled using anti-PECAM-1 conjugated to Alexa 488 (10 μ g/ml, local perfusion) and anti-CD11a conjugated to Alexa 488 (3 μ g/ml, i.v). Time lapsed microscopy ($\times 90$) was used to quantify the number of transmigrating leukocytes at each location. (A) % of total leukocytes that underwent TEM at the junctional region (junc) or via transcellular route (non-junc). When the route could not be clearly assigned to either pathway it was assigned to “un-assg”. (B) The fraction of adhered leukocytes that underwent TEM was determined in straight and converging regions. (C) Leukocyte TEM at bi-cellular (bi) and tri-cellular (tri) junctions, as well as at non-junctional (non) regions as percentage of the total leukocytes that underwent TEM in straight and converging regions. In panels A-C white bars represent straight and black bars represent converging regions. For all groups in panels A-C n=188 leukocytes were tracked in 9 straight and 148 leukocytes in 7 converging regions, in 5 mice. Bars are mean+SE. ***/[^] Significantly different from each other or others in same group (p<0.001), ** Significantly different from each other (p<0.01). (D) Representative image sequence demonstrating leukocyte initial adhesion location, the crawling route, and TEM during 125 sec time period. The white arrows track leukocyte displacement. The black arrow above the images indicates the flow direction. The bar is 12 μ m.

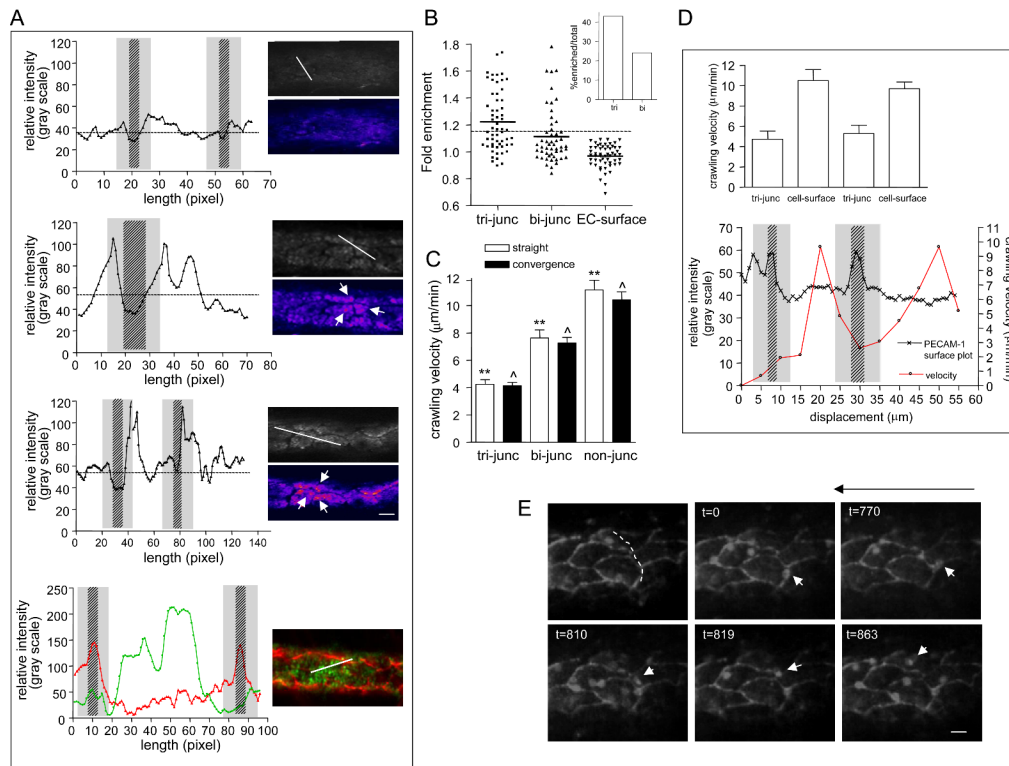


Figure 6. Enrichment of ICAM-1 near tri-cellular EC junctions is associated with slower leukocyte crawling in these regions

In separate experiments ICAM-1 distribution and leukocyte crawling velocities near EC-junctions were quantified. (A,B) Venular ECs were stained for ICAM-1 using anti-ICAM-1 (YN/1.7.4, 50 μ g/ml, local perfusion) and fluorescently tagged secondary (anti-rat Alexa 488, 50 μ g/ml, local perfusion) antibodies in sequence. (A) Representative raw and pseudocolored images (on the right) depict ICAM-1 enrichment near tri-cellular junctions post fMLP superfusion (second from the top) and following 4 hours TNF α activation (third from the top), but not under control conditions (upper images). Corresponding ICAM-1 fluorescence intensity profiles (on the left) were obtained along the projected white line shown on the raw images. The lines were placed on the ECs that had the best focus in the field of view, and that encompassed one or more tri-cellular junctions. White arrows on the images of venules from fMLP and TNF α activated tissue indicate ICAM-1 enriched regions near tri-cellular junctions. The broken line on each intensity plot is the mean relative intensity, the patterned areas indicate the width of the junction and the gray regions represent 5 μ m wide regions extending on both sides of the outlined junction. Similarly, selected venules were stained for P-selectin (in green, RB40.34, 50 μ g/ml followed by anti-rat Alexa 488, 50 μ g/ml) and PECAM-1 (in red, ER-MP12-PE, Ebioscience, 10 μ g/ml) after fMLP superfusion. Bottom panel (Fig 6a) depicts a representative image and a corresponding intensity plot (out of n=28 cells), where the relative, corresponding intensities of junctional PECAM-1 (red) and surface P-selectin (green) were obtained along the projected white line. Unlike ICAM-1, P-selectin is not enriched near EC-junctions. (B) Measurements of relative ICAM-1 expression (as a function of relative fluorescence intensity) near tri-cellular junctions (tri-junc), bi-cellular junctions (bi-junc) and random regions on EC-surface away from EC-junctions (EC-surface) were performed as described in Methods. Intensities that were 2 SD higher than the mean intensity of randomly measured ROIs on EC surface (above the dotted line) were defined as enriched regions. The insert shows percent of enriched tri- and bi-cellular junctions out of the total number of sampled junctions (n=58 tri- and 55 bi-cellular junctions, 5 venules from 3 mice). Approximately 43%

of all tri-cellular junctions and only 23% of all bi-cellular junctions were enriched in ICAM-1. (C-E) EC-junctions and interacting leukocytes were immunofluorescently labeled using anti-PECAM-1 conjugated to Alexa 488 (10 μ g/ml, local perfusion) and anti-CD11a conjugated to Alexa 488 (3 μ g/ml, i.v). Time lapsed microscopy (\times 90) was used to track crawling leukocytes in straight regions and venular convergences 50 minutes post fMLP superfusion. (C) Leukocyte crawling velocities over tri-cellular junctions (tri-junc), bi-cellular junctions (bi-junc) including the 5 μ m wide region on both sides of the junction were measured and compared to crawling velocities on the non-junctional regions (non-junc). (D) In the bottom panel, crawling velocity of a representative leukocyte was tracked in consecutive 5- μ m lengths of EC surface while the leukocyte remained in focus. The trajectory of the crawling leukocyte was traced (white dashed line, E, upper left panel) and the intensity plot along that line (left y-axis) was superimposed on the velocity plot (right y-axis). The patterned areas on the intensity plot show the locations of the two tri-cellular junctions that the leukocyte encountered on this path and the gray areas are regions of 5- μ m width on both sides of the outlined junction; these are regions of the lowest leukocyte crawling velocity. (D) upper panel shows average crawling velocity of all tracked cells (n=7, 5 mice) in each of the regions shown in the representative trace (bottom panel). Crawling velocities over tri-cellular junctions were significantly slower compared to bi-cellular junctions or non-junctional regions, consistent with the ICAM-1 enrichment shown in panel B. (E) Image sequence demonstrating the initial location of a representative leukocyte and its crawling route during 863 seconds. The white arrows track the leukocyte displacement. Long arrow above the image indicates the direction of flow. The bar is 10 μ m. **/^ Significantly different from each other (p<0.01).

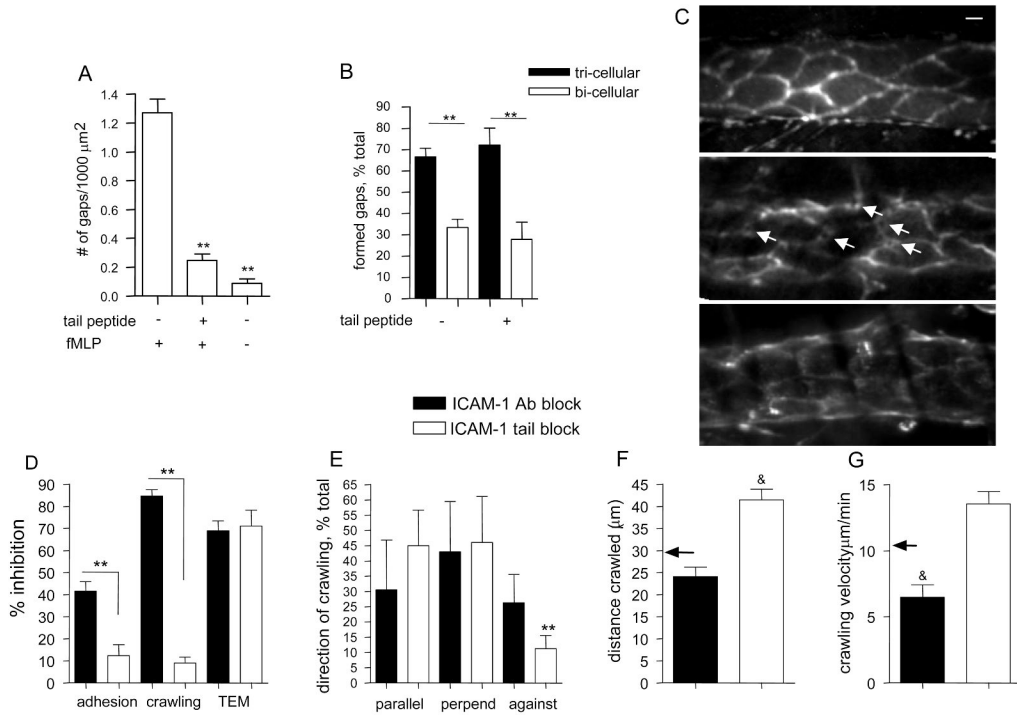


Figure 7. Blockade of either the luminal or the cytoplasmic domains of ICAM-1 reduces leukocyte TEM via different mechanisms

(A-C) VE-Cadherin distribution. (A) Venules were stained for VE-Cadherin (anti-VE-Cadherin, BV13, 30 $\mu\text{g}/\text{ml}$ local intraluminal perfusion). The formation of gaps in VE-Cadherin per field of view was quantified with or without fMLP (after 50 minutes, 10 μM , superfusion) and ICAM-1 tail peptide (100 $\mu\text{g}/\text{ml}$, local cannulation) as indicated. All measurements were normalized to 1000 μm^2 . (B) The location of the formed gaps in VE-Cadherin was quantified with respect to EC-junctions in the presence or absence of ICAM-1 tail peptide. Formation of “gaps” in VE-Cadherin was significantly attenuated in the presence of ICAM-1 tail peptide, but did not alter the distribution of those that formed, as the majority (~70%) remained at tri-cellular junctions. (C) EC-junctions stained for VE-Cadherin were observed immediately upon completion of the cannulation protocol (a representative image is shown in the upper panel, control conditions) and then again 50 minutes post fMLP application (a representative image is shown in the middle panel). Control images of VE-Cadherin and 50 minutes post fMLP application in the presence of either ICAM-1 tail peptide (a representative image is shown in the bottom panel) or control-penetratin peptide (not shown) were collected. As shown by white arrows (middle panel), fMLP application to the tissue resulted in formation of a large number of gaps in VE-Cadherin. When used, the penetratin-peptides were added immediately following control data collection, but prior to fMLP superfusion. For all groups in panels A-C n=4 mice, 7 venules for each condition. To quantify leukocyte-EC interactions (panels D-H) EC junctions and leukocytes were immunofluorescently labeled using anti-PECAM-1 conjugated to Alexa 488 (10 $\mu\text{g}/\text{ml}$, local perfusion) and anti-CD11a conjugated to Alexa 488 (3 $\mu\text{g}/\text{ml}$, i.v). All observations were made 50 minutes post fMLP application (10 μM , superfusion) in the presence of either ICAM-1 blocking antibody (YN/1.7.4, 50 $\mu\text{g}/\text{ml}$), ICAM-1 tail peptide (100 $\mu\text{g}/\text{ml}$), or control peptide (100 $\mu\text{g}/\text{ml}$), which were introduced intraluminally by local cannulation. (D) Leukocyte adhesion (leukocytes/80 μm vessel length), crawling (fraction of total adhered) and TEM (leukocytes/10000 μm^2 extravascular tissue). n=4 mice, 7 venules. The residual fraction of crawling leukocytes in ICAM-1 Ab blocking and ICAM-1 tail peptide experiments was quantified for directionality (E), distance (F) and

crawling velocity (G). In F and G the black arrows indicate the average crawling distance and crawling velocity (respectively) as shown in Figure 4 in the absence of peptide treatment. ** Significantly different from each other or others in the same group ($p < 0.001$). & Significantly different from values shown in figure 4 in the absence of peptide treatment ($p < 0.05$). Control peptide did not prevent the formation of gaps in VE-Cadherin and did not decrease leukocyte TEM (not shown), suggesting role for ICAM-1 signaling in leukocyte TEM. The bar in panel C is $10\mu\text{m}$.

Table 1
Dimensions of ECs in straight and converging venular regions

Venular region	EC length (μm)	EC width (μm)	Area (μm^2)	Aspect ratio	Orientation (degrees)	N
region 3 (straight)	52.3 \pm 1.1*	16.6 \pm 0.4	879.9 \pm 18.2*	0.34 \pm 0.01**	10.6 \pm 1.8**	102
region 1 (convergence)	38.2 \pm 0.8*	16.9 \pm 0.3	593.8 \pm 23.6*	0.46 \pm 0.02**	17.8 \pm 1.8**	89

Values are means \pm SE. EC-junctions in selected venules were immunofluorescently labeled for PECAM-1. The major and minor axis as well as EC area were calculated using ImageJ software. EC aspect ratio is presented as (width/length). EC orientation is the angle of EC major axis relative to the axial direction.

* Significantly different from each other ($p < 0.01$),

** ($p < 0.001$)